α-tubulin nuclear overexpression is an indicator of poor prognosis in patients with non-Hodgkin's lymphoma

SHINICHI HAYASHI[1], TETSUO MIKAMI[2], YOSHIHIRO MURAI[3], YASUO TAKANO[4] and JOHJI IMURA[1]

[1]Department of Diagnostic Pathology, Graduate School of Medicine and Pharmaceutical Sciences, University of Toyama, Toyama 930-0194; [2]Department of Pathology, Toho University School of Medicine, Ota, Tokyo 143-8540; [3]Department of Nursing, Toyama College of Welfare Science, Imizu 939-0341; [4]Kanagawa Cancer Center Research Institute, Asahi, Yokohama 241-8515, Japan

Received December 23, 2013; Accepted April 16, 2014

DOI: 10.3892/ijmm.2014.1793

Abstract. In the present study, the newly established mouse monoclonal antibody, Y-49, binding to a specific epitope of α-tubulin, was used to examine immunohistochemical reactivity in 116 patients with non-Hodgkin's lymphoma (NHL). The protein was detected at elevated levels in the nuclei of human proliferating cells by western blot analysis, flow cytometry and immunohistochemical analysis. The relatively weak binding in the cytoplasm was evident in almost all cases. The investigation of the correlation between immunohistochemical positivity and clinicopathological variables revealed links with the MIB-1 proliferation index and poor survival. Nuclear positivity with Y-49 was more frequent in older-aged patients, those with nodal NHL and in those who harbored the diffuse large B-cell histological subtype, and was strongly associated with high MIB-1 labeling indices (LIs). Survival analysis by the Kaplan-Meier method revealed statistically significant differences between patients with high and low Y-49 LIs (p=0.0181), even in the group with advanced (stage III/IV) disease (p=0.0327). Multivariate analysis revealed that overexpression of α-tubulin is an independent prognostic factor in NHL with a relative risk of 2.786.

Introduction

In the present study, we produced a mouse monoclonal antibody, Y-49, against synthesized polypeptides with 17 amino acids selected from the published survivin sequence (1). However, the anbitody detects α-tubulin, with a very similar amino acid sequence, and we found intense immunoreactivity in tumor cell nuclei to be linked with a poor prognosis of patients with non-Hodgkin's lymphoma (NHL).

Correspondence to: Dr Johji Imura, Department of Diagnostic Pathology, Graduate School of Medicine and Pharmaceutical Sciences, University of Toyama, 2630 Sugitani, Toyama 930-0194, Japan
E-mail: imura@med.u-toyama.ac.jp

Key words: α-tubulin, proliferative activity, prognostic factor, non-Hodgkin's lymphoma

Tubulin subunits of microtubules (MTs), i.e., cylindrical organelles found in almost all eukaryote cells, which are involved in a number of cellular processes, including mitosis, cilia and flagella motility and the intracellular transport of vesicles and organelles (2), are mainly composed of heterodimers of two polypeptides designated as α and β (3). γ-tubulin is required for the initiation of MT assembly and it is found at the minus end of MTs (4). Over the years, four new members of the tubulin family, δ, ε, ζ and η, have been identified; however, their cellular functions are yet to be fully established (5-9). α- and β-tubulin are encoded by a family of genes that produces polypeptides which differ primarily in the C-terminal variable domain, which consists of 15 amino acids (10), and have several isotypes (2). In mammalians, the class III β-tubulin isotype is expressed in a differentiation-dependent manner in human neuroblastic tumors, such as medulloblastomas (11), retinoblastomas (12) and peripheral neuroblastomas (13). In addition, a corresponding epitope has been detected in cases of squamous cell carcinoma, lymphoma and melanoma (14). As regards the specificity of α-tubulin isotypes, six isotypes have been identified and found to be distributed in various organs (15). However, to the best of our knowledge, no study on the expression of α-tubulin in malignant tumors has been published to date.

Materials and methods

Production of Y-49 antibody. Using the published survivin sequence (1), a 17-amino acid oligopeptide was synthesized, conjugated with Freund's incomplete adjuvant, and then injected into female BALB/c mice intraperitoneally three times at 10-day intervals for immunization. After boosting, splenocytes were fused with P3x63-Ag8653 mouse myeloma cells and hybridomas were grown in RPMI-1640 medium supplemented with 10% fetal calf serum and were then subcloned twice. The supernatants were screened for reactivity with the original antigens and one positive line was named Y-49.

Western blot anlaysis. Two cultured cell lines, Raji (Burkitt's lymphoma) and MKN28 (gastric cancer), were purchased from Riken Cell Bank, Tsukuba, Japan. A total of 1-10x10^6 cultured cells and two samples of normal lymphocytes

obtained from tonsils resected for chronic tonsillitis were homogenized in 0.01 M phosphate-buffered saline (PBS) and centrifuged (19,000 x g, 30 min). The supernatants were mixed with 62.5 mM Tris-HCl buffer, pH 6.8, containing 2% sodium dodecyl sulfate (SDS), 5% 2-mercaptoethanol, 7% glycerol and 0.01% bromophenol blue, and then boiled for 10 min. Proteins (10 μg aliquots) were electrophoresed on 8% SDS-polyacrylamide gels at 30 mA for 3 h, and transferred onto 0.45 mm polyvinylidene fluoride (PVDF) membranes (Immobilon-P, Millipore, Bedford, MA, USA), using a semi-dry system (Biocraft, Tokyo, Japan) at 200 mA for 30 min. The membranes were blocked with 5% skimmed milk in PBS and then incubated with Y-49 (dilution, x200), α-tubulin (Neomarkers, Westinghouse, CA, USA; DM1A, x200) and HSP90 (Medical and Biological Laboratories, Nagoya, Japan) antibodies at 4˚C overnight, followed by exposure to horseradish peroxidase-conjugated rabbit anti-mouse immunoglobulin-G (IgG; Dako, Copenhagen, Denmark). Specific binding was determined by enhanced chemiluminescence (Amersham, Buckinghamshire, UK) on X-ray films (RX-U; Fuji, Tokyo, Japan). All procedures for western blot analysis were repeated in triplicate for confirmation.

Immunoprecipitation. Immunoprecipitation was performed according to previously described methods (16). The Raji cell samples (50 mg) were washed twice with ice-cold PBS, homogenized in 1 ml of IP buffer (50 mM HEPES; 150 mM NaCl, 0.1 mM phenyl-methylsulfonyl fluoride, 20 U/ml aprotinin, pH 8.0) and centrifuged at 14,000 x g for 3 min. Protein G-Sepharose (30 μl) was added to the supernatant followed by rotation at 4˚C for 30 min. Following centrifugation at 5,000 x g for 1 min, 0.5 μg of antibody were added to the supernatant followed by rotation at 4˚C for 1 h. Subsequently, 30 ml of protein G-Sepharose wee introduced with rotation at 4˚C for 30 min. The sediments were washed with ice-cold IP buffer three times under the same conditions (3,000 x g, 5 min, 4˚C). The same volume of 2X SDA sample buffer was added to the sediment solution and the resultant preparations were used for western blot analysis. The antibodies employed for immunoprecipitation were the following: Y-49, DM1A (α-tubulin), β-tubulin (Neomarkers) and HSP90.

Cell fractionation. Cell fractionation was performed as previously described (17). A total of $4x10^6$ NHL cells were collected after rinsing with cold STE (100 mM NaCl, 10 mM Tris, 1 mM EDTA, pH 7.4) and centrifuged at 1,000 x g for 5 min. Following the addition of 0.8 ml hypotonic lysis buffer (10 mM Tris, 0.2 mM Mg, pH 7.4) to the pellet and gentle vortexing, the cells were broken open by with 30 strokes in a Dounce homogenizer followed by the addition of 200 μl 1.25 M sucrose and 2 μl 0.5 M EDTA. Following centrifugation at 1,000 x g for 10 min, the supernatant (S1) was removed to an ultracentrifuge tube and the pellet was resuspended with 1 ml solution of 0.25 M sucrose, 10 mM Tris, 1 mM EDTA, pH 7.4, homogenized ten strokes, and centrifuged at 1,000 x g for 10 min. The pellet, which was designated as the P1 fraction, was enriched with nuclei. The supernatant S1 was removed and further centrifuged at 100,000 x g for 1 h to yield the supernatant S100 fraction, containing cytosolic proteins. A fraction enriched in mitochondrial membranes could be obtained by centrifuging S1 at 10,000 x g for 10 min. Finally, western blot analysis was performed on each fraction as described above.

Analysis of amino acid sequences. Amino acid sequence analysis was performed by the in-gel digestion method described by Rosenfeld *et al* (18). After immunoprecipitation and western blot analysis employing Y-49, in-gel-digested protein bands stained with Coomassie brilliant blue were excised and washed twice with 150 μl of 50% acetonitrile in 200 mM ammonium carbonate (pH 8.9) for 20 min at 30˚C in an Eppendorf tube. The gel slices were partially rehydrated with 5 μl of 200 mM ammonium carbohydrate, 0.02% Tween-20 (pH 8.9). Subsequently, 2 μl of porcine trypsin solution (250 μg/ml in ammonium carbonate, pH 8.9) were added. After the absorption of the protease solution, 5 μl of ammonium carbonate buffer were added together with a minimum volume of rehydration buffer, which was added to totally immerse the gel slices. The digestion was carried out for 4 h at 30˚C and then terminated by the addition of 1.5 μl of fluoroacetic acid. The resulting peptides were recovered by two extractions of 20 min each, with 100 μl of a solution of 60% acetonitrile, 0.1% trifluoroacetic acid, at 30˚C with shaking in an Ependorf thermomixer.

The peptides eluted from the polyacrylamide matrices were separated using C18 Brownlee reverse-phase columns (Brownlee Labs, Santa Clara, CA, USA) and were eluted with a linear gradient of acetonitrile, 0.1% trifluoroacetic acid at a flow rate of 0.3 ml/min with the Brownlee Labs micro-gradient system. Elution was monitored at 218 nm with a Spectroflow 783 programmable absorbance detector (Kratos Analytical Ltd., Manchester, UK), and peaks were manually collected. N-terminal sequence analysis was performed on a gas-phase sequencer (470A; Applied Biosystems).

Immunofluorescence double staining. Immunofluorescence double staining was employed for the demonstration of the localization of Y-49 binding antigens. Formalin-fixed, paraffin-embedded fibrin-clots obtained from two NHL cell lines were prepared and cut into 4 μm-thick sections. Y-49 (dilution, x100) and Ki-67 (Dako; dilution, x1) were used as primary antibodies and anti-mouse IgG conjugated with fluorescein Texas red (FITC; Dako; dilution, x200) and anti-rabbit IgG conjugated with fluorescein isothiocyanate (FITC; Dako; dilution, x200) were utilized as the respective secondary antibodies. The sections in these cases were not treated with the microwave oven heating method, as this often results in overstaining. All preparations were examined under a confocal microscope (model LSM-GB200; Olympus, Tokyo, Japan), equipped with argon and argon-krypton lasers. Details of the staining and confocal microscopy procedures have been described in a previous study (19).

Flow cytometry. Normal lymphocytes obtained from healthy volunteers were incubated at 37˚C for 96 h under stimulation with phytohemagglutinin (PHA, 5 μg/ml) and fixed for 40 min with paraformaldehyde solution (0.5 g/ml) in PBS at 4˚C and were washed and subsequently permeabilized with 0.1% Triton X-100 in PBS. Following incubation with Y-49, DM1A (α-tubulin) and HSP90 at 4˚C for 1 h, the lymphocytes were washed and labeled with fluorescein isothiocyanate goat anti-mouse serum for 30 min. An IgG2b antibody (Dako) was used

as the negative control. Cytometry was performed on a FACScan flow cytometer (Becton-Dickinson, Mountain View, CA, USA), DNA staining being recorded on a linear scale and antibody staining on a log scale. A total of 1,024 channels were analyzed.

Immunohistochemistry. Formalin-fixed, paraffin-embedded tissue blocks were available for each case. Sections cut at 4 μm thickness were stained with the standard labeled streptavidin-biotin-peroxidase method (LSAB kit; Dako) to investigate the localization and degree of reactivity with Y-49 (dilution, x100), α-tubulin (Clone DM1A, dilution, x100) and MIB-1 against the Ki-67 antigen (Dako; dilution, x100), all being mouse monoclonal antibodies. Prior to the immunohistochemical procedures, the sections were placed in heat-resistant plastic staining jars containing an antigen-retrieval solution, 10 mM citric acid with pH 6.0 (Wako, Osaka, Japan), heated in a microwave oven for 5 min at 500 W three times, and then allowed to cool to room temperature. Finally, color was developed at the sites of reactivity with a substrate kit followed by counterstaining with Meyer's hematoxylin. The immunohistochemical control procedure, employed in conjunction with all the methods described above, consisted of the replacement of the primary antibodies with an equivalent amount of normal mouse IgG (Dako). Negative results were thereby obtained in all instances. Tonsil, esophagus and stomach tissues were also employed for the evaluation of Y-49 and DM1A in normal tissues.

Assessment of reactivity for Y-49 and MIB-1. In the present study, we focused on Y-49 positivity in nuclei since weak Y-49 cytoplasmic positivity was noted in almost all cases examined. Overexpression in nuclei was determined by counting immunoreactive cells in >1,000 NHL cells in high-power, microscope images of representative sections in each case. A cut-off value was defined from the results of histograms for positive cells among all examined cases as detailed in Results, and the cases were divided into two groups, with high and low labeling indices (LIs). LIs for MIB-1 staining were calculated in a similar manner, with counts of >1,000 cells. The cases were again subdivided into two groups with high and low indices.

Patients examined. Data from 116 patients for whom a diagnosis of NHL was made on the basis of clinical, radiological and histological examinations were randomly retrieved from the patient files at Kitasato University Hospital (Sagamihara, Japan) and Toyama University Hospital (Toyama, Japan). Reviewing the available tissue slides in each case, the histological subtypes of NHL were determined by two of the authors (S.H. and Y.T.), according to the criteria established by the Revised European and American Lymphoma (REAL) Study Group (20).

Clinical information was obtained from the patient files. All the patients underwent appropriate chemo- and/or radiotherapy shortly after the establishment of the final diagnosis.

Study approval. The study complied with the Declaration of Helsinki and the Local Ethics Committee of the University of Toyama (Toyama, Japan) approved the research protocol. Written informed consent was obtained from each participant. Animal care and surgical procedures were in accordance with the 'Principles of Laboratory Animal Care' prepared by the National Academy of Sciences.

Statistical analysis. Statistical analyses were performed using the program StatView J 5.0 for Windows. All values shown are the means ± standard error (SE), unless otherwise stated. Correlations of categorical variables were analyzed using the χ^2 test. To compare the distributions of continuous variables in the two groups, the Mann-Whitney U test was utilized. Survival analysis was performed by the Kaplan-Meier method with the log-rank test and the Cox multivariate method. Differences were considered statistically significant when the p-value was <0.05.

Results

Western blot analysis, immunoprecipitation and cell fractionation. Western blot analysis with Y-49 demonstrated one strong band of approximately 57 kDa and one weak band of approximately 90 kDa in the Raji and MKN28 cells and normal lymphocytes (Fig. 1A, lanes 1-3). The intensity of the 57 kDa band in the normal lymphocytes was less than that in the Raji and NKM28 cells. With DM1A, only clear single bands of approximately 57 kDa were evident in the samples (Fig. 1A, lanes 4-6). With HSP90, clear bands of approximately 90 kDa were observed (Fig. 1A, lanes 7-9). Western blot analysis of the Raji cells revealed clear single bands, with DM1A after immunoprecipitation using Y-49 or HSP90, but not with β-tubulin (Fig. 1B, lanes 1-3). Furthermore, the binding of Y-49 after immunoprecipitation using DM1A and HSP90 was detected (Fig. 1B, lanes 4-6). Cell fractionation revealed a clear band of approximately 57 kDa in the nuclear fraction (Fig. 1C, lanes 1 and 4), two bands of approximately 57 and 90 kDa in the cytoplasmic fraction (Fig. 1C, lane 3) and a clear band of approximately 57 kDa in the mitochondrial fraction. Immunoprecipitation confirmed no presence of HSP90 in the nuclear fraction.

Analysis of amino acid sequence. Amino acid sequence analysis of the 57 kDa protein band revealed a ten polypeptide sequence from the N-terminus 'Val-Gly-Ile-Asn-Tyr-Gln-Pro-Pro-Thr-Val', identical to a stretch of α-tubulin (The Swiss Institute of Bioinformatics and the EMBL outstation - The European Bioinformatics Institute). Amino acid sequence analysis of the 90-kDa protein demonstrated a ten polypeptide sequence from the N-terminus 'Ile-Arg-Tyr-Glu-Ser-Leu-Thr-Asp-Pro-Ser', identical to part of HSP90 (The Swiss Institute of Bioinformatics and the EMBL outstation - The European Bioinformatics Institute).

Immunofluorescence double staining. Fig. 2 demonstrates the results of the immunofluorescence double staining of Y-49 and Ki-67. The red color, Y-49, was visible in both the nuclei and the cytoplasm (Fig. 2A) and the green color, showing positivity of Ki-67, was found restricted to nuclei (Fig. 2B). The yellow color indicated the double staining of Y-49 and Ki-67. There was a great deal of overlap as shown by double staining (Fig. 2C), but Y-49-positive cells were slightly more frequent than Ki-67-positive cells.

Flow cytometry. Fig. 3A shows the results of flow cytometric with Y-49, 96 h following PHA stimulation. The vertical axis represents the cell count and the horizontal axis the fluorescent intensity, two major peaks being recognized. After

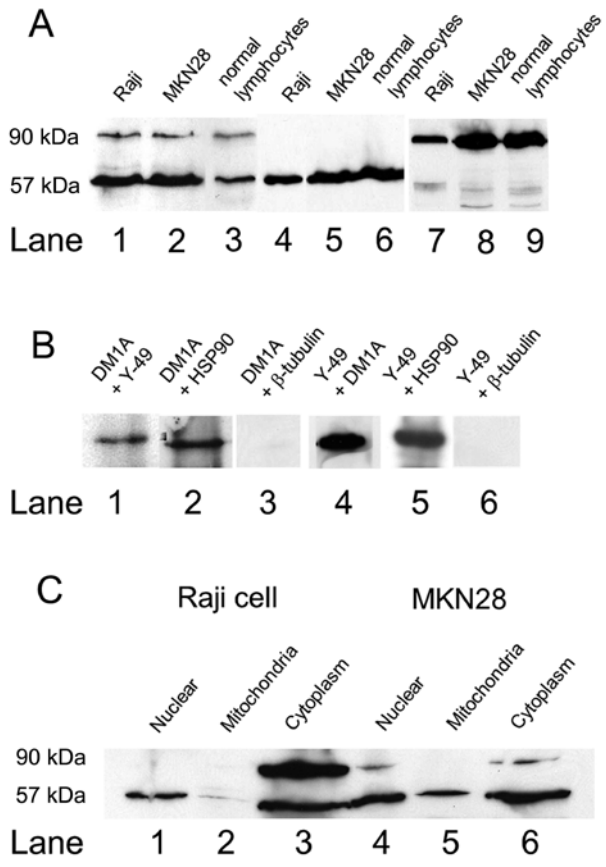

Figure 1. (A) Western blot analysis for Y-49. One strong clear band of approximately 57 kDa and one weak, but clear band of approximately 90 kDa are present in the supernatants from the Raji and MKN28 cells and normal lymphocytes. The intensity of the 57 kDa band in normal lymphocytes is less than that in the Raji and NKM28 cells (lanes 1-3). Note the single band of approximately 57 kDa with DM1A samples (lanes 4-6) and weak but clear bands of approximately 90 kDa with HSP90 (lanes 7-9). (B) Immunoprecipitation between Y-49, DM1A and HSP90 in Raji cells. Western blot analysis of clear single bands with DM1A after immunoprecipitation using Y-49 and HSP90, but not with β-tubulin (lanes 1-3). Binding Y-49 after immunoprecipitation using DM1A and HSP90 is also apparent (lanes 4-6). (C) Western blot analysis for fractions of Raji cells. Note the clear band of approximately 57 kDa in the nuclear fraction (lanes 1 and 4), two bands around the site of 57 and 90 kDa in the cytoplasmic fraction (lane 3) and at a clear one band of approximately 57 kDa in the mitochondrial fraction.

Table I. Clinical and histopathological characteristics of the 116 patients with non-Hodgkin's lymphoma.

	Y-49 labeling indices (LIs)			
Characteristic	Total (%)	High (%)	Low (%)	p-value
Median age (years)	55 (9-90)	59 (9-90)	49 (10-83)	0.1827
Gender				0.9553
Male	67 (57.8)	40 (59.7)	27 (40.3)	
Female	49 (42.2)	29 (59.2)	20 (40.8)	
T/B lineage				0.4256
T-cell	30 (25.9)	16 (53.3)	14 (46.7)	
B-cell	86 (74.1)	53 (61.6)	33 (38.4)	
Primary site				0.0031
Nodal	81 (69.8)	41 (50.6)	40 (49.4)	
Extranodal	35 (30.2)	28 (80.0)	7 (20.0)	
Histological subtype				0.0005
Diffuse large B	60 (51.7)	47 (78.3)	13 (21.7)	
Follicle center	13 (11.2)	2 (15.4)	11 (84.6)	
T-cell lymphoma	30 (25.9)	16 (53.3)	14 (46.7)	
Others	13 (11.2)	4 (30.8)	9 (69.2)	
Tumor stage				0.4939
I/II	54 (46.6)	34 (63.0)	20 (37.0)	
III/IV	60 (51.7)	34 (56.7)	26 (43.3)	
Unknown	2 (1.7)	1 (50.0)	1 (50.0)	
Therapy				
Chemotherapy	109 (94.0)			
Radiation	54 (46.6)			
No therapy	4 (3.4)			
Response to therapy				0.6424
Complete/ partial response	91 (81.3)	57 (62.4)	34 (37.6)	
No response	16 (14.3)	9 (56.3)	7 (43.8)	
Unknown	5 (4.5)	2 (40.0)	3 (60.0)	

gating analysis, cells of the left peak were found to be 2N in accordance with G0/G1 (Fig. 3B) and cells of the right peak demonstrated entrance into the cell cycle (Fig. 3C). The results with DM1A and HSP90 at 96 h after stimulation revealed one peak, as shown in Fig. 3A (left), showing 2N on gating.

Immunohistochemistry of normal tissues. Tonsil, esophagus and stomach samples were used to determine the distribution of Y-49-positive cells in normal tissues. The cells in the dark zone of germinal centers, harboring proliferating cells, were strongly positive (Fig. 4A), and suprabasal epithelial cells of the esophageal epithelium (Fig. 4B) and the cells in the neck zone of the gastric epithelium (Fig. 4C) also demonstrated a positive reaction. By contrast, DM1A positivity was almost restricted to the cytoplasm, although diffusely in almost all cells.

Clinical characteristics. The data for clinical and histological characteristics are summarized in Table I. The age of the patients ranged from 9 to 90 years (median, 55 years); 67 were males and 49 were females. Immunohistochemistry of the NHLs revealed that 30 cases were of the T-cell lineage and 86 of the B-cell lineage. The primary site was nodal in 81 patients and extranodal in 35 patients. The tumor stages were early (stage I/II) in 54 patients, advanced (stage III/IV) in 60 patients and unknown in 2 patients. According to the REAL classification, the cases were subclassified into 60 cases of diffuse large B-cell lymphoma, 13 cases of follicle center cell lymphoma and 30 cases of T-cell type lymphoma, the remaining 13 being of other subtypes (Table I). Shortly after diagnosis, chemo- and/or radiotherapy were performed in 112 patients. Such therapy was effective in 91 cases.

Immunohistochemistry for NHL cases. The reaction for Y-49 was strong in the nuclei in the positive NHL cases, but present in the cytoplasm in almost all cases. Therefore, we did not devote further attention to the cytoplasmic positivity.

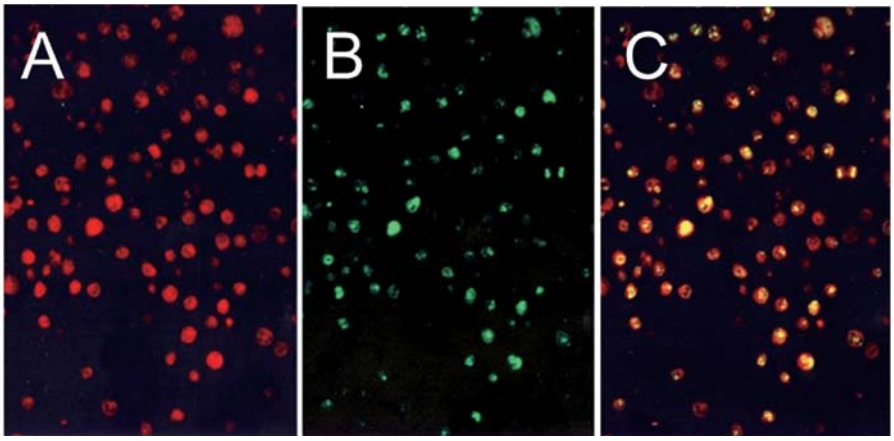

Figure 2. Immunofluorescence double staining of Y-49 and Ki-67. The red color, showing positivity of Y-49, is visible in both nuclei and cytoplasm (A), while the green color, for Ki-67, is found restricted to nuclei (B). The yellow color indicates double staining of Ki-67 and Y-49. Y-49-positive cells are slightly more frequent than Ki-67-positive cells (C).

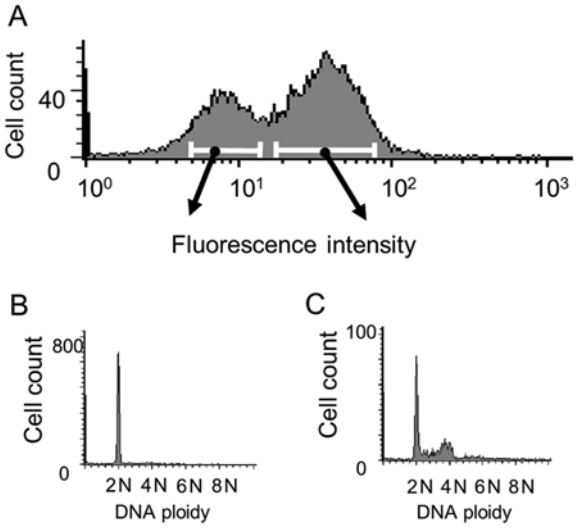

Figure 3. Flow cytometric analysis of PHA stimulated normal lymphocytes. (A) Results with Y-49 96 h after PHA stimulation. (B) After gating analysis, cells of the left peak are 2N in accordance with G0/G1. (C) Cells of the right peak are distributed from 2N to 6N.

Histograms of Y-49 LIs for NHL cases, demonstrating two major peaks, are shown in Fig. 5. The cut-off value was determined as the trough LI (25.0) between the two peaks.

The results for Y-49 immunoreactivity in relation to the LIs for MIB-1 were significantly correlated ($p<0.0001$). Microscopic features are shown in Fig. 6. On the basis of histogram results of the LIs for Y-49, 47 (40.5%) and 69 (59.5%) of the 116 cases were subdivided into groups with high and low LIs, respectively. Cases of the diffuse large B-cell type were more likely to have high LIs for Y-49 and MIB-1 than the other histological subtypes. DM1A staining demonstrated no linkage to either Y-49 or MIB-1 staining.

Survival and evaluation of clinicopathological variables in relation to reactivity for Y-49. The overexpression of Y-49 binding proteins was associated with older age ($p=0.00348$), an extranodal primary site ($p=0.0003$) and the diffuse large B-cell type histological subtype ($p<0.0001$). The other clinicopathologic variables did not show any significant correlation with Y-49 (Table I). MIB-1 LIs did not correlate with any of the variables examined in this study.

Follow-up data were available for all patients. Overall survival ranged from 1 to 107 months, with a median of 28 months. With univariate analyses of all variables, older age (>65 years, $p=0.0460$), tumor stage (I/II vs. III/IV, $p=0.0006$), response to chemo- and radiotherapy (CR/PR vs. none, $p<0.0001$) and reactivity for Y-49 (high vs. low, $p=0.0183$) showed strong correlations with overall survival. Survival analysis by the Kaplan-Meier method revealed significant differences in survival at 23 months between patients with and without overexpression of Y-49 binding proteins ($p=0.0181$; Fig. 7A). When the NHL cases were divided into three groups according to a Y-49 LI higher than the mean + 1/2 standard deviation (SD), within the mean ± 1/2 SD and lower than the mean - 1/2 SD, the Kaplan-Meier method also revealed significant differences ($p=0.0067$; Fig. 7B). In late-stage NHL cases, a higher Y-49 LI was also associated with a poorer prognosis ($p=0.0327$; Fig. 7C). High MIB-1 LIs tended to be positively linked with survival, although this was not statistically significant ($p=0.1605$). The other clinicopathological variables did not show any meaningful correlation with survival.

Multivariate analysis to identify prognostic factors for survival was performed for 107 patients as follows: first, all variables listed in Table I were defined as baseline factors; then, Cox model forward and backward selection procedures were applied to identify which of the four variables described above were most strongly associated with survival for the patients. All of the four variables proved to be independent prognostic factors (Table II). Response to therapy and reactivity for Y-49 demonstrated significant links with the survival of the patients. By contrast, DM1A positivity had no association with the survival of NHL patients.

Discussion

The present study indicated that α-tubulin expression in NHL may play an important role in patient survival. The mouse monoclonal antibody, Y-49, was newly raised against a synthe-

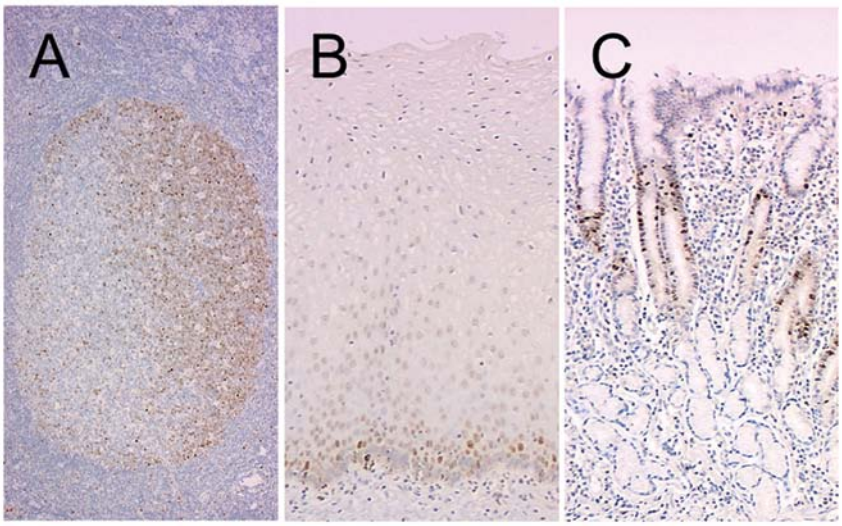

Figure 4. Distribution of Y-49-positive cells in normal tissues. Nuclei of cells (A) in the dark zone of germinal centers, (B) in the suprabasal epithlium of the esophagus and (C) in the neck zone of the gastric epithelium demonstrate a positive reaction.

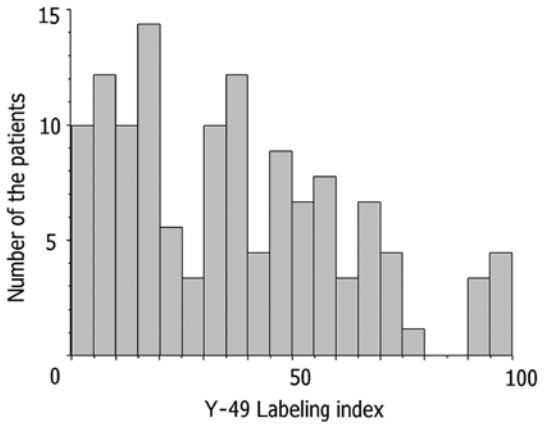

Figure 5. Histograms of Y-49 labeling indices (LIs) for non-Hodgkin's lymphoma (NHL) cases, demonstrating two major peaks.

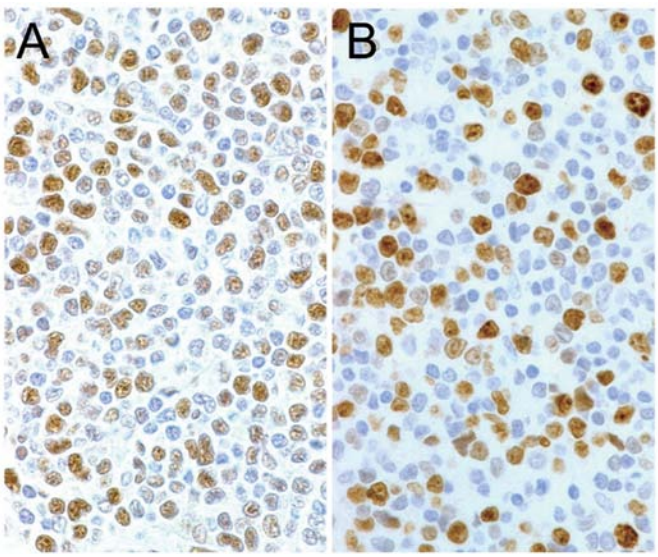

Figure 6. (A) In a formalin-fixed tissue section from a diffuse large B-cell type lymphoma, more than half the atypical cells show a nuclear reaction with Y-49 (x600). (B) Nuclear reaction for MIB-1 (x600) in the same area of a semi-serial section.

Table II. Results of multivariate Cox analysis in 107 patients with non-Hodgkin's lymphoma.

	Relative risk	95% CI[a]	p-value
Response to therapy	5.814	2.770-12.20	<0.0001
Overexpression of Y-49	2.786	1.389-5.590	0.0039
Stage of tumor	2.530	1.270-5.040	0.0083
Age (≥65 years)	1.957	1.048-3.650	0.0349

CI, confidence interval.

sized 17-amino acid polypeptide based on the survivin amino acid sequence as an immunogen. When examined by FASTA of the National Center of Biotechnology Information (21), this polypeptide showed no homology with already known proteins apart from survivin. However, it appears that the antibody also recognizes antigens completely unrelated to the survivin molecule.

In the present study, a high Y-49 LI closely correlated with the poor prognosis of patients with NHL, both for all cases and advanced cases alone (stage III/IV). Among the clinical and histopathological variables examined in the present study, only old age, tumor stage, status of therapeutic response and the overexpression of Y-49 binding proteins in the nuclei were found to be independent prognostic factors, the latter two showing the most significant correlations with survival. Moreover, Y-49 LIs were strongly associated with proliferative activity, as assessed by MIB-1 labeling. Indeed, Y-49 reacted with proliferating cells, such as those in the dark zone of germinal centers, esophageal supurabasal epithelial cells and gastric neck zone epithelial cells, of normal tissues as observed in previous studies for Ki-S2 (22), Ki-67 (23) and proliferating cell nuclear antigen (PCNA) (24). Similar results were also obtained from flow cytometric analysis, indicating Y-49-positive cells to have entered the cell cycle, although

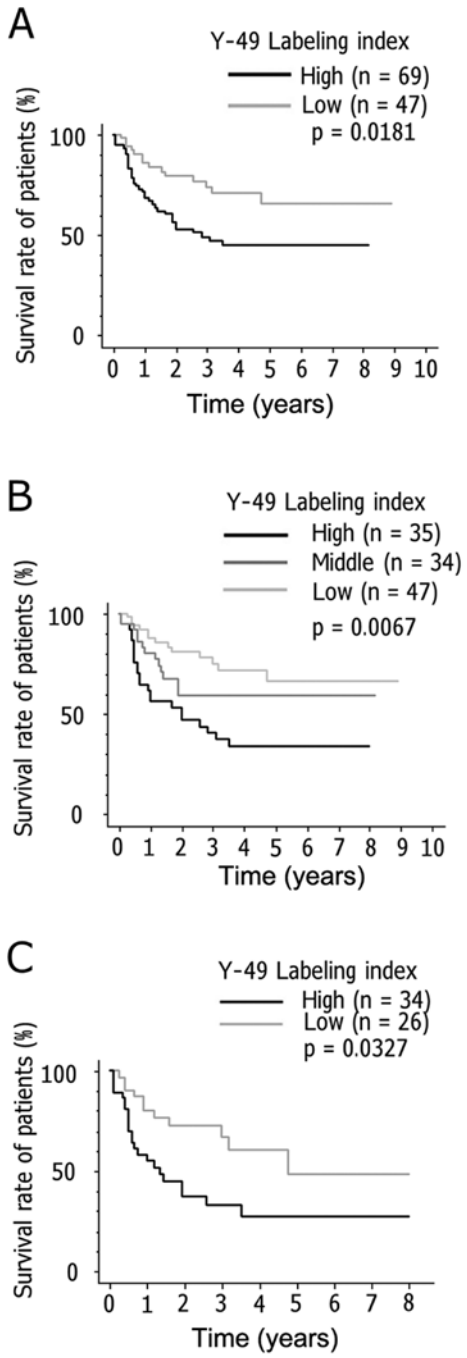

Figure 7. Kaplan-Meier survival curves according to the labeling indices (LIs) for Y-49 in 116 patients with non-Hodgkin's lymphoma. (A) Total cases divided into high and low Y-49 LIs groups. (B) Total cases were divided into three groups according to a Y-49 LI higher than the mean + 1/2 SD, within the mean ± 1/2 SD and the mean - 1/2 SD. (C) Late-stage cases divided into high and low Y-49 LIs groups.

the background noise of HSP90 and DM1A needs to be carefully considered. There are many proliferation-associated nuclear antigens, such as Ki-S2, Ki-67, PCNA and the laminin receptor, whose overexpression is closely associated with the poor survival of patients with malignant lymphomas and other malignant epithelial tumors (25-29). Based on the present results, it can be concluded that α-tubulin also plays a role in survival. Whether this is directly linked to proliferation remains to be determined.

While the overexpressed molecule in the nuclei stained with Y-49 was shown to be α-tubulin by cell fractionation and western blot analysis, a commercially available α-tubulin monoclonal antibody (Clone DM1A) detected varying amounts in the cytoplasm, but seldom demonstrated any nuclear binding. The difference in reactivity from Y-49 is presumably due to the antigen isotype, of which α-tubulin has six, differentially distributed (15). For example, α1 is mostly found in the brain and the lungs, less often in the testes, and even less often in the heart, kidneys, muscle, spleen, stomach and thymus (30). By contrast, α3/7 is expressed only in the testes at very high levels (30), whereas α2 follows a similar pattern to α1 (31). There may be a functional significance, but this has not been established yet (2). Generally, tubulin molecules are subjected to a large number of post-translational modifications, such as phosphorylation, acetylation, tyrosination, polyglutamylation and polyglycylation, positively or negatively related to the regulation of MT assembly, MT stabilization and the cell cycle (2,32). In activated human B-lymphocytes, α-tubulin appears to be phosphorylated on a tyrosine residue near the C terminus by the tyrosine kinase, Syk (33). Acetylation appears to occur following incorporation into MTs, inducing an increase in their stabilization (34). Tyrosinated and non-tyrosinated α-tubulin often form different MTs in the same cell; the former is common in the interphase network and in the spindle, while the non-tyrosinated form occurs in some interphase MTs (35). DM1A was produced through the immunization of native chick brain microtubules and recognizes an epitope in the parts of the C terminal region of the α-tubulin (36). It is considered that the differences between α-tubulin detected by Y-49 and DM1A are derived from variations in the recognized epitopes and/or post-translational modifications.

Y-49 also recognizes HSP90, albeit only weakly. This may be only a cross-reaction, but it has been reported that HSP90 can bind to tubulin and inhibit its polymerization (37). In the present study, immunoprecipitation proved the binding of HSP90 and α-tubulin. Thus, our data suggest that Y-49 detects the epitope of α-tubulin which binds to HSP90.

Acknowledgements

This study was supported in part by a Grant-in-Aid for Scientific Research from the Ministry of Education, Science, Sports, Culture and Technology of Japan.

References

1. Ambrosini G, Adida C and Altieri DC: A novel anti-apoptosis gene, survivin, expressed in cancer and lymphoma. Nat Med 3: 917-921, 1997.
2. Luduena RF: Multiple forms of tubulin: different gene products and covalent modifications. Int Rev Cytol 178: 207-275, 1998.
3. Dutcher SK: The tubulin fraternity: alpha to eta. Curr Opin Cell Biol 13: 49-54, 2001.
4. Schiebel E: γ-tubulin complexes: binding to the centrosome, regulation and microtubule nucleation. Curr Opin Cell Biol 12: 113-118, 2000.
5. Dutcher SK and Trabuco E: The UN13 gene is required for the assembly of basal bodies in Chlamydomonas and encodes delta tubulin, a new member of the tubulin superfamily. Mol Biol Cell 9: 1293-1308, 1998.
6. Ruiz F, Garreau de Lobresse N and Beisson J: A mutation affecting basal body duplication and cell shape in Paramecium. J Cell Biol 104: 417-430, 1987.

7. Ruiz F, Krzywicka A, Klotz C, *et al*: The SM19 gene, required for duplication of basal bodies in *Paramecium*, encodes a novel tubulin, eta-tubulin. Curr Biol 10: 1451-1454, 2000.
8. Chang P and Stearns T: δ- and ε-tubulin: two new human centrosomal tubulins reveal new aspects of centrosome structure and function. Nat Cell Biol 2: 30-35, 2000.
9. Vaughn S, Attwood T, Navarro M, Scott V, McKean P and Gull K: New tubulins in protozoal parasites. Curr Biol 10: R258-R259, 2000.
10. Draberova E, Lukas Z, Ivanyi D, Viklicky V and Draber P: Expression of class III β-tubulin in normal and neoplastic human tissues. Histochem Cell Biol 109: 231-239, 1998.
11. Katsetos CD, Herman MM, Frankfurter A, *et al*: Cerebellar desmoplastic medulloblastomas. A further immunohistochemical characterization of the reticulin-free pale islands. Arch Pathol Lab Med 113: 1019-1029, 1989.
12. Katsetos CD, Herman MM, Frankfurter A, Uffer S, Perentes E and Rubinstein LJ: Neuron-associated class III β-tubulin isotype, microtubule-associated protein 2, and synaptophysin in human retinoblastomas in situ. Further immunohistochemical observations on the Frlexner-Wintersteiner rosettes. Lab Invest 64: 45-54, 1991.
13. Katosetos CD, Karkavelas G, Frankfurter A, *et al*: The stromal Schwann cell during maturation of peripheral neuroblastomas: immunohistochemical observations with antibodies to the neuronal class III beta-tubulin isotype (beta III) and S-100 protein. Clin Neuropathol 13: 171-180, 1994.
14. Scott CA, Walker CC, Neal DA, *et al*: Beta-tubulin epitope expression in normal and malignant epithelial cells. Arch Otolaryngol Head Neck Surg 116: 583-589, 1990.
15. Lewis SA and Cowan NJ: Complex regulation and functional versatility of mammalian α- and β-tubulin isotypes during differentiation of testis and muscle cells. J Cell Biol 106: 2023-2033, 1988.
16. Murai Y, Dobashi Y, Okada E, Ishizawa S, Shiota M, Mori S and Takano Y: Study on the role of G1 cyclins in Epstein-Barr virus-associated human lymphomas maintained in severe combined immune deficiency (SCID) mice. Int J Cancer 92: 232-239, 2001.
17. Okamura H, Sigal CT, Alland L and Resh MD: Rapid high-resolution western blotting. Methods Enzymol 254: 535-550, 1995.
18. Rosenfeld J, Capdevielle J, Guillemot JC and Ferrara P: In-gel digestion of proteins for internal sequence analysis after one- or two- dimensional gel electrophoresis. Anal Biochem 203: 173-179, 1992.
19. Matsui K, Jin XM, Kitagawa M and Miwa A: Clinicopathologic features of neuroendocrine carcinoma of the stomach: appraisal of small-cell and large-cell variants. Arch Pathol Lab Med 122: 1010-1017, 1998.
20. Harris NL, Jaffe ES, Stein H, *et al*: A revised European-American classification of lymphoid neoplasms: a proposal from the International Lymphoma Study Group. Blood 84: 1361-1392, 1994.
21. Pearson WR and Lipman DJ: Imported tools for biological sequence comparison. Proc Natl Acad Sci USA 85: 2444-2448, 1988.
22. Heidebrecht HJ, Buck F, Steinmann J, Sprenger R, Wacker HH and Parwaresch R: p100: a novel proliferation-associated nuclear protein specifically restricted to cell cycle phases S, G2 and M. Blood 90: 226-233, 1997.
23. Reynolds GM, Rowlands DC and Mead GP: Detection of Ki-67 antigen by a new sheep polyclonal antiserum. J Clin Pathol 48: 1138-1140, 1995.
24. Shibahara K and Stillman B: Replication-dependent marking of DNA by PCNA facilitates CAF-1-coupled inheritance of chromatin. Cell 96: 575-585, 1999.
25. Sabattini E, Gerdes J, Gherlinzoni F, *et al*: Comparison between the monoclonal antibodies Ki-67 and PC10 in 125 malignant lymphomas. J Pathol 169: 397-403, 1993.
26. Suzuki H: Expression of the 67-KD laminin-binding protein in human lymphomas. Hum Pathol 30: 361-362, 1999.
27. Rudolph P, Alm P, Heidebrecht HJ, *et al*: Immunologic proliferation marker Ki-S2 as prognostic indicator for lymph node-negative breast cancer. J Natl Cancer Inst 91: 271-278, 1999.
28. Fontanini G, Vignati S, Chiné S, *et al*: 67-Kilodalton laminin receptor expression correlates with worse prognostic indicators in non-small cell carcinomas. Clin Cancer Res 3: 227-231, 1997.
29. Waltregny D, De Leval L, Ménard S, De Leval J and Castronovo V: Independent prognostic value of the 67-kd laminin receptor in human prostate cancer. J Natl Cancer Inst 89: 1224-1227, 1997.
30. Lewis SA and Cowan NJ: Tubulin genes: structure, expression, and regulation. Avilla J (eds). In: Microtubule Proteins. CRC Press, Boca Raton, FL, pp37-66, 1990.
31. Przyborski SA and Cambray-Deakin MA: Developmental regulation of α-tubulin mRNAs during the differentiation of cultured cerebellar granule cells. Brain Res Mol Brain Res 36: 179-183, 1996.
32. MacRae TH: Tubulin post-translational modifications: enzymes and their mechanisms of action. Eur J Biochem 244: 265-278, 1997.
33. Peters JD, Furlong MT, Asai DJ, Harrison ML and Geahlen RL: Syk, activated by cross-linking the B-cell antigen receptor, localizes to the cytosol where it interacts with and phosphorylates α-tubulin on tyrosine. J Biol Chem 271: 4755-4762, 1996.
34. Wilson PJ and Forer A: Acetylated α-tubulin in spermatogenic cells of the crane fly Nephrotoma suturalis: kinetochore microtubules are selectively acetylated. Cell Motil Cytoskeleton 14: 237-250, 1989.
35. Gumdersen GG, Kalmoski MH and Bulinski JC: Distinct populations of microtubules: tyrosinated and nontyrosinated alpha tubulin are distributed differently in vivo. Cell 38: 779-789, 1984.
36. Breitling F and Little M: Carboxy-terminal regions on the face of tubulin and microtubules. Epitope locations of YOL1/34, DM1A and DM1B. J Mol Biol 189: 367-370, 1986.
37. Garnier C, Barbier P, Gilli R, Lopez C, Peyrot V and Briand C: Heat-shock protein 90 (hsp90) binds in vitro to tubulin dimmer and inhibits microtubule formation. Biochem Biophys Res Commun 250: 414-419, 1998.